"Nonlocal" Diffusion Coefficients for Neutronic Systems Containing Voided Subregions

Edward W. Larsen[*], Jim E. Morel[†], Jijie Lou[†]

[*]*Department of Nuclear Engineering and Radiological Sciences, University of Michigan, Ann Arbor, MI 48104*
[†]*Department of Nuclear Engineering, Texas A&M University, College Station, TX 77843*
edlarsen@umich.edu, morel@tamu.edu, loujijie1991@tamu.edu

Abstract - *This paper presents a systematic derivation of space-dependent diffusion coefficients for neutronically diffusive 3D systems with anisotropic scattering that contain "small" voided subregions. The resulting diffusion coefficients in a solid homogeneous part of the physical system reduce to the standard $D = 1/3\Sigma_t$. However, for spatial points in or near a void region, the diffusion coefficient becomes a space-dependent 3×3 anisotropic tensor, which can be obtained by solving a 3D transport problem without scattering. The resulting anisotropic diffusion theory should be valid if the void regions are sufficiently small that they perturb, but do not significantly alter, the "diffusive" character of the system.*

I. INTRODUCTION

In many nuclear reactor problems, an approximate neutron diffusion simulation is employed as an alternative to a more expensive neutron transport simulation. Several generalizations of the classic diffusion approximation have been developed to extend the range of this approximation. For example, *homogenized* diffusion approximations are widely used to simulate heterogeneous reactor lattices, and *Simplified P_N* approximations (coupled systems of diffusion equations) are used for other problems in which transport effects cannot be completely ignored. However, all standard diffusion-based approximations have a specific difficulty when the physical system contains a void subregion in which the total cross section $\Sigma_t(x)$ is 0: the diffusion coefficient $D(x) = 1/3\Sigma_t(x)$ becomes infinite. The infinite diffusion coefficient can render the diffusion approximation invalid, even if the void regions occupy a small fraction of the physical system and the basic "diffusive" character of the system remains intact. The principal issue is that standard diffusion coefficients are not properly defined in void regions.

The problem of formulating finite, accurate diffusion coefficients for diffusive neutronic systems containing voided subregions has been considered previously, for special geometries [1, 2, 3]. However, a more general approach has recently been developed for infinite heterogeneous-medium problems with isotropic scattering, and successfully tested for finite heterogeneous-medium problems [4, 5, 6]. This method systematically replaces the traditional "local" diffusion coefficient at a point x, $D(x) = 1/3\Sigma_t(x)$, by a "nonlocal" diffusion tensor, which "averages" the values of $\Sigma_t(x')$, with points x' near x generally weighted more heavily. The method is now being considered for use in simulating the soon-to-restart TREAT reactor at INL. The method also has been successfully tested as a transport accelerator, for problems containing void subregions [7].

In the present paper, we provide a theoretical derivation of the method for monoenergetic finite-medium neutron transport k-eigenvalue problems, with linearly anisotropic scattering and vacuum boundary conditions. (Previous derivations treated only infinite medium problems with isotropic scattering [4, 5, 6].) Most importantly, the boundary conditions systematically derived here – for functions needed to construct the nonlocal diffusion tensors – are new, and are identical to the boundary conditions found experimentally to be most efficient in [7]. This congruence of experiment and theory is consistent with the fact that these boundary conditions should yield the most accurate diffusion solutions.

The remainder of this summary is organized as follows. In Section II the basic problem is introduced, and preliminary results are stated. In Section III the principal new theoretical result – the "nonlocal" diffusion tensor – is derived. In Section IV our theoretical results are summarized, and in the final Section V, we discuss computational results.

II. PROBLEM DESCRIPTION

We consider a monoenergetic k-eigenvalue problem, prescribed for a finite, heterogeneous, fissile system V with linearly anisotropic scattering:

$$\Omega \cdot \nabla \psi(x,\Omega) + \Sigma_t(x)\psi(x,\Omega) = \frac{1}{4\pi}\Big(\Sigma_{s0}(x)\phi(x)$$
$$+ 3\Sigma_{s1}(x)\Omega \cdot J(x) + \frac{1}{k}\nu\Sigma_f(x)\phi(x)\Big),$$
$$x \in V, \ \Omega \in 4\pi, \quad (1a)$$
$$\psi(x,\Omega) = 0, \ x \in \partial V, \ \Omega \cdot n < 0, \quad (1b)$$

where

$$\phi(x) = \int_{4\pi} \psi(x,\Omega')d\Omega' = \text{ scalar flux}, \quad (2a)$$

$$J(x) = \int_{4\pi} \Omega'\psi(x,\Omega')d\Omega' = \text{ neutron current}. \quad (2b)$$

Operating on Eq. (1a) by $\int_{4\pi}(\cdot)d\Omega$, we obtain the *neutron balance equation*:

$$\nabla \cdot J(x) + \Sigma_t(x)\phi(x) = \Big(\Sigma_{s0}(x) + \frac{1}{k}\nu\Sigma_f(x)\Big)\phi(x). \quad (3)$$

The classic diffusion approximation to Eq. (1a) consists of the exact balance Eq. (3), with the approximate *Fick's Law*:

$$J(x) = -D(x)\nabla\phi(x), \quad (4a)$$

where

$$D(\boldsymbol{x}) = \frac{1}{3\Sigma_t(\boldsymbol{x})} = \textit{diffusion coefficient} . \qquad (4b)$$

Eqs. (4) can be derived by the classic P_1 approximation, in which it is assumed that

$$\psi(\boldsymbol{x}, \boldsymbol{\Omega}) = \frac{1}{4\pi}\big(\phi(\boldsymbol{x}) + 3\boldsymbol{\Omega} \cdot \boldsymbol{J}(\boldsymbol{x})\big) + \cdots , \qquad (5)$$

where "$\cdots$" refers to terms that are formally small and ignored. Eqs. (4) and (5) can also be rigorously derived by an asymptotic expansion with a small parameter ε, in which

$$\phi(\boldsymbol{x}) = O(1) , \qquad (6a)$$
$$\boldsymbol{J}(\boldsymbol{x}) = O(\varepsilon) , \qquad (6b)$$
$$\boldsymbol{\nabla} = O(\varepsilon) , \qquad (6c)$$

and

$$\text{Eq. (5) holds with "} \cdots \text{''} = O(\varepsilon^2) . \qquad (6d)$$

Again, the formal P_1 and the asymptotic approaches both yield Eqs. (4), in which $D(\boldsymbol{x})$ becomes infinite when $\Sigma_t(\boldsymbol{x}) = 0$. In this situation, the underlying assumptions of the P_1 and asymptotic theories are not met; both theories become invalid.

The method proposed in this paper does not assume that Eq. (5) is valid. More precisely: *it does not require ψ to be nearly a linear function of $\boldsymbol{\Omega}$ for all directions of flight*. However, *it does assume that Eqs. (6a), (6b), and (6c) hold*. This will happen if ψ has weak spatial derivatives and is nearly a linear function of $\boldsymbol{\Omega}$ – except possibly for a small "cone" of directions $\boldsymbol{\Omega}$ in which O(1) deviations from Eq. (5) can occur. [These directions would correspond to the directions of flight along a narrow voided channel in V. The channel can have an O(1) effect on ψ for this small cone of directions – but if it has a sufficiently small effect on $\phi(\boldsymbol{x})$ and $\boldsymbol{J}(\boldsymbol{x})$, then Eqs. (6a), (6b), and (6c) can all hold. This is the scenario envisioned here.]

The approach taken in this paper requires the formulation, from Eqs. (1), of suitable equations for $\phi(\boldsymbol{x})$ and $\boldsymbol{J}(\boldsymbol{x})$, in which the assumptions (6a), (6b), and (6c) can be systematically applied. One of these equations is the exact neutron balance Eq. (3). A second exact equation relating $\phi(\boldsymbol{x})$ and $\boldsymbol{J}(\boldsymbol{x})$ is derived next.

III. THE NONLOCAL DIFFUSION TENSOR

As a preamble to the analysis of Eqs. (1), let us consider the problem

$$\boldsymbol{\Omega} \cdot \boldsymbol{\nabla} f(\boldsymbol{x}, \boldsymbol{\Omega}) + \Sigma_t(\boldsymbol{x})f(\boldsymbol{x}, \boldsymbol{\Omega}) = g(\boldsymbol{x}, \boldsymbol{\Omega}) ,$$
$$\boldsymbol{x} \in V , \ \boldsymbol{\Omega} \in 4\pi , \qquad (7a)$$
$$f(\boldsymbol{x}, \boldsymbol{\Omega}) = 0 , \ \boldsymbol{x} \in \partial V , \ \boldsymbol{\Omega} \cdot \boldsymbol{n} < 0 , \qquad (7b)$$

where $g(\boldsymbol{x}, \boldsymbol{\Omega})$ is any specified function. The exact solution $f(\boldsymbol{x}, \boldsymbol{\Omega})$, obtained using the method of characteristics, is

$$f(\boldsymbol{x}, \boldsymbol{\Omega}) = \int_0^{\ell(\boldsymbol{x}, \boldsymbol{\Omega})} e^{-\int_0^s \Sigma_t(\boldsymbol{x}-s'\boldsymbol{\Omega})ds'} g(\boldsymbol{x} - s\boldsymbol{\Omega}, \boldsymbol{\Omega})ds$$
$$\equiv (\boldsymbol{\Omega} \cdot \boldsymbol{\nabla} + \Sigma_t)^{-1}g(\boldsymbol{x}, \boldsymbol{\Omega}) , \ \boldsymbol{x} \in V , \ \boldsymbol{\Omega} \in 4\pi , \quad (8)$$
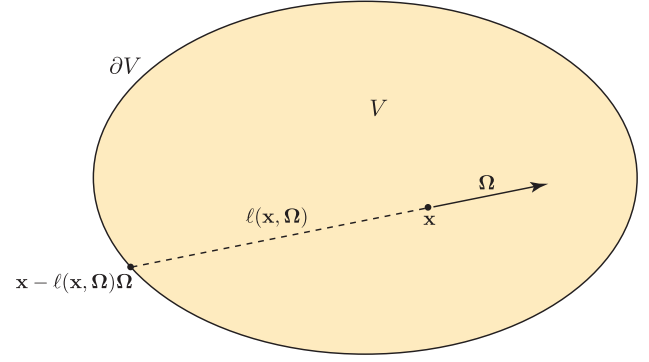

Fig. 1: The System V and the Function $\ell(\boldsymbol{x}, \boldsymbol{\Omega})$.

where

$$\ell(\boldsymbol{x}, \boldsymbol{\Omega}) = \text{the distance from } \boldsymbol{x} \text{ to } \partial V$$
$$\text{in the direction } -\boldsymbol{\Omega} \text{ (see Fig. 1)} \qquad (9a)$$

is the solution of the problem

$$\boldsymbol{\Omega} \cdot \boldsymbol{\nabla}\ell(\boldsymbol{x}, \boldsymbol{\Omega}) = 1 , \ \boldsymbol{x} \in V , \ \boldsymbol{\Omega} \in 4\pi , \qquad (9b)$$
$$\ell(\boldsymbol{x}, \boldsymbol{\Omega}) = 0 , \ \boldsymbol{x} \in \partial V , \ \boldsymbol{\Omega} \cdot \boldsymbol{n} < 0 . \qquad (9c)$$

We emphasize that the line integral operator $(\boldsymbol{\Omega} \cdot \boldsymbol{\nabla} + \Sigma_t)^{-1}$ defined in Eq. (8) maps any function $g(\boldsymbol{x}, \boldsymbol{\Omega})$ into a function $f(\boldsymbol{x}, \boldsymbol{\Omega})$ that satisfies the boundary condition (7b). For this reason, $(\boldsymbol{\Omega} \cdot \boldsymbol{\nabla} + \Sigma_t)^{-1}$ is only a one-sided inverse of $\boldsymbol{\Omega} \cdot \boldsymbol{\nabla} + \Sigma_t$. Specifically, $\boldsymbol{\Omega} \cdot \boldsymbol{\nabla} + \Sigma_t$ and $(\boldsymbol{\Omega} \cdot \boldsymbol{\nabla} + \Sigma_t)^{-1}$ satisfy:

$$(\boldsymbol{\Omega} \cdot \boldsymbol{\nabla} + \Sigma_t)(\boldsymbol{\Omega} \cdot \boldsymbol{\nabla} + \Sigma_t)^{-1}g(\boldsymbol{x}, \boldsymbol{\Omega}) = g(\boldsymbol{x}, \boldsymbol{\Omega}) , \qquad (10a)$$

and

$$(\boldsymbol{\Omega} \cdot \boldsymbol{\nabla} + \Sigma_t)^{-1}(\boldsymbol{\Omega} \cdot \boldsymbol{\nabla} + \Sigma_t)g(\boldsymbol{x}, \boldsymbol{\Omega})$$
$$= \int_0^{\ell(\boldsymbol{x}, \boldsymbol{\Omega})} e^{-\int_0^s \Sigma_t(\boldsymbol{x}-s'\boldsymbol{\Omega})ds'}\big(\boldsymbol{\Omega} \cdot \boldsymbol{\nabla} + \Sigma_t(\boldsymbol{x} - s\boldsymbol{\Omega})\big)g(\boldsymbol{x} - s\boldsymbol{\Omega}, \boldsymbol{\Omega})ds$$
$$= \int_0^{\ell(\boldsymbol{x}, \boldsymbol{\Omega})} e^{-\int_0^s \Sigma_t(\boldsymbol{x}-s'\boldsymbol{\Omega})ds'}\big(-\frac{d}{ds} + \Sigma_t(\boldsymbol{x} - s\boldsymbol{\Omega})\big)g(\boldsymbol{x} - s\boldsymbol{\Omega}, \boldsymbol{\Omega})ds$$
$$= -\int_0^{\ell(\boldsymbol{x}, \boldsymbol{\Omega})} \frac{d}{ds}\big(e^{-\int_0^s \Sigma_t(\boldsymbol{x}-s'\boldsymbol{\Omega})ds'} g(\boldsymbol{x} - s\boldsymbol{\Omega}, \boldsymbol{\Omega})\big)ds$$
$$= -e^{-\int_0^s \Sigma_t(\boldsymbol{x}-s'\boldsymbol{\Omega})ds'} g(\boldsymbol{x} - s\boldsymbol{\Omega}, \boldsymbol{\Omega})\Big|_0^{\ell(\boldsymbol{x}, \boldsymbol{\Omega})}$$
$$= g(\boldsymbol{x}, \boldsymbol{\Omega}) - e^{-\int_0^{\ell(\boldsymbol{x}, \boldsymbol{\Omega})} \Sigma_t(\boldsymbol{x}-s'\boldsymbol{\Omega})ds'} g(\boldsymbol{x} - \ell(\boldsymbol{x}, \boldsymbol{\Omega})\boldsymbol{\Omega}, \boldsymbol{\Omega}) .$$
$$(10b)$$

To proceed with the analysis of Eqs. (1), we use Eq. (3) to rewrite Eq. (1a) as

$$\boldsymbol{\Omega} \cdot \boldsymbol{\nabla}\psi(\boldsymbol{x}, \boldsymbol{\Omega}) + \Sigma_t(\boldsymbol{x})\psi(\boldsymbol{x}, \boldsymbol{\Omega})$$
$$= \frac{1}{4\pi}\Big[\Sigma_t(\boldsymbol{x})\phi(\boldsymbol{x}) + \boldsymbol{\nabla} \cdot \boldsymbol{J}(\boldsymbol{x}) + 3\Sigma_{s1}(\boldsymbol{x})\boldsymbol{\Omega} \cdot \boldsymbol{J}(\boldsymbol{x})\Big]. \quad (11)$$

Next, using Eqs. (7)-(10), we write the solution $\psi(\boldsymbol{x}, \boldsymbol{\Omega})$ of Eqs. (11) and (1b) as:

$$\psi(\boldsymbol{x}, \boldsymbol{\Omega}) = \frac{1}{4\pi}(\boldsymbol{\Omega} \cdot \boldsymbol{\nabla} + \Sigma_t)^{-1}\Big[\Sigma_t\phi + \boldsymbol{\nabla} \cdot \boldsymbol{J} + 3\Sigma_{s1}\boldsymbol{\Omega} \cdot \boldsymbol{J}\Big]$$
$$= \frac{1}{4\pi}(\boldsymbol{\Omega} \cdot \boldsymbol{\nabla} + \Sigma_t)^{-1}\Big[(\boldsymbol{\Omega} \cdot \boldsymbol{\nabla} + \Sigma_t)\phi + \boldsymbol{\nabla} \cdot \boldsymbol{J}$$
$$- \boldsymbol{\Omega} \cdot (\boldsymbol{\nabla}\phi - 3\Sigma_{s1}\boldsymbol{J})\Big]$$
$$= \frac{1}{4\pi}(\boldsymbol{\Omega} \cdot \boldsymbol{\nabla} + \Sigma_t)^{-1}(\boldsymbol{\Omega} \cdot \boldsymbol{\nabla} + \Sigma_t)\phi$$
$$+ \frac{1}{4\pi}(\boldsymbol{\Omega} \cdot \boldsymbol{\nabla} + \Sigma_t)^{-1}\boldsymbol{\nabla} \cdot \boldsymbol{J}$$
$$- \frac{1}{4\pi}(\boldsymbol{\Omega} \cdot \boldsymbol{\nabla} + \Sigma_t)^{-1}\boldsymbol{\Omega} \cdot (\boldsymbol{\nabla}\phi - 3\Sigma_{s1}\boldsymbol{J})$$
$$= \frac{1}{4\pi}\Big[\phi(\boldsymbol{x}) - e^{-\int_0^{\ell(x,\Omega)}\Sigma_t(x-s'\Omega)ds'}\phi\big(\boldsymbol{x} - \ell(\boldsymbol{x}, \boldsymbol{\Omega})\boldsymbol{\Omega}\big)\Big]$$
$$+ \frac{1}{4\pi}(\boldsymbol{\Omega} \cdot \boldsymbol{\nabla} + \Sigma_t)^{-1}\boldsymbol{\nabla} \cdot \boldsymbol{J}$$
$$- \frac{1}{4\pi}(\boldsymbol{\Omega} \cdot \boldsymbol{\nabla} + \Sigma_t)^{-1}\boldsymbol{\Omega} \cdot (\boldsymbol{\nabla}\phi - 3\Sigma_{s1}\boldsymbol{J}) . \quad (12)$$

Operating on Eq. (12) by $\int_{4\pi} \boldsymbol{\Omega}(\cdot)d\Omega$ yields:

$$\boldsymbol{J}(\boldsymbol{x}) = -\frac{1}{4\pi}\int_{4\pi}\boldsymbol{\Omega}\Big(e^{-\int_0^{\ell(x,\Omega)}\Sigma_t(x-s'\Omega)ds'}\Big)\phi\big(\boldsymbol{x} - \ell(\boldsymbol{x}, \boldsymbol{\Omega})\boldsymbol{\Omega}\big)d\Omega$$
$$+ \frac{1}{4\pi}\int_{4\pi}\boldsymbol{\Omega}(\boldsymbol{\Omega} \cdot \boldsymbol{\nabla} + \Sigma_t)^{-1}\boldsymbol{\nabla} \cdot \boldsymbol{J}(\boldsymbol{x})\,d\Omega$$
$$- \frac{1}{4\pi}\int_{4\pi}\boldsymbol{\Omega}(\boldsymbol{\Omega} \cdot \boldsymbol{\nabla} + \Sigma_t)^{-1}\boldsymbol{\Omega} \cdot \big(\boldsymbol{\nabla}\phi(\boldsymbol{x}) - 3\Sigma_{s1}\boldsymbol{J}(\boldsymbol{x})\big)d\Omega .$$
$$(13)$$

To this point no approximations have been made; Eq. (13), like the neutron balance Eq. (3), is exact.

Eqs. (3) and (13) are the basis of the new nonlocal tensor diffusion approximation. To derive this approximation, we retain the exact Balance Eq. (3), and we suitably approximate each of the three integrals on the right side of Eq. (13) to obtain a generalization of Fick's Law.

The first integral,

$$\boldsymbol{J}_1(\boldsymbol{x}) = -\frac{1}{4\pi}\int_{4\pi}\boldsymbol{\Omega}\Big(e^{-\int_0^{\ell(x,\Omega)}\Sigma_t(x-s'\Omega)ds'}\Big)\phi\big(\boldsymbol{x} - \ell(\boldsymbol{x}, \boldsymbol{\Omega})\boldsymbol{\Omega}\big)d\Omega$$
$$(14a)$$

has an integrand that is defined in terms of values of the scalar flux $\phi(\boldsymbol{x}')$ for points $\boldsymbol{x}' = \boldsymbol{x} - \ell(\boldsymbol{x}, \boldsymbol{\Omega})\boldsymbol{\Omega} \in \partial V$. (In fact, this integral can be converted to a surface integral over $\boldsymbol{x}' \in \partial V$.) Since ψ satisfies a vacuum boundary condition on ∂V and the system V is diffusive, then $\phi(\boldsymbol{x}')$ is small for $\boldsymbol{x}' \in \partial V$. Also, for most points $\boldsymbol{x}' \in \partial V$, these small values of $\phi(\boldsymbol{x}')$ are exponentially attenuated from $\boldsymbol{x}' \in \partial V$ to $\boldsymbol{x} \in V$ – making the integral even smaller. For these reasons, we choose to ignore this term:

$$\boldsymbol{J}_1(\boldsymbol{x}) \approx 0 . \quad (14b)$$

The second integral on the right side of Eq. (13) is:

$$\boldsymbol{J}_2(\boldsymbol{x}) = \frac{1}{4\pi}\int_{4\pi}\boldsymbol{\Omega}(\boldsymbol{\Omega} \cdot \boldsymbol{\nabla} + \Sigma_t)^{-1}\boldsymbol{\nabla} \cdot \boldsymbol{J}(\boldsymbol{x})\,d\Omega . \quad (15a)$$

By Eqs. (6), $\boldsymbol{J}_2 = O(\varepsilon^2)$, which is smaller than $\boldsymbol{J} = O(\varepsilon)$. Consequently, we choose to ignore this term as well:

$$\boldsymbol{J}_2(\boldsymbol{x}) \approx 0 . \quad (15b)$$

In the third integral on the right side of Eq. (13), we appeal to Eqs. (6) to get for small s

$$\boldsymbol{\nabla}\phi(\boldsymbol{x} - s\boldsymbol{\Omega}) = \boldsymbol{\nabla}\phi(\boldsymbol{x}) + O(\varepsilon^2 s) ,$$
$$\boldsymbol{J}(\boldsymbol{x} - s\boldsymbol{\Omega}) = \boldsymbol{J}(\boldsymbol{x}) + O(\varepsilon^2 s) .$$

Thus, we obtain with $O(\varepsilon^2)$ error,

$$\boldsymbol{J}_3(\boldsymbol{x}) = -\frac{1}{4\pi}\int_{4\pi}\boldsymbol{\Omega}\int_0^{\ell(x,\Omega)}\Big(e^{-\int_0^s\Sigma_t(x-s'\Omega)ds'}\Big)$$
$$\boldsymbol{\Omega} \cdot \Big[\boldsymbol{\nabla}\phi(\boldsymbol{x} - s\boldsymbol{\Omega}) - 3\Sigma_{s1}(\boldsymbol{x} - s\boldsymbol{\Omega})\boldsymbol{J}(\boldsymbol{x} - s\boldsymbol{\Omega})\Big]ds\,d\Omega$$
$$\approx -\frac{1}{4\pi}\int_{4\pi}\boldsymbol{\Omega}\int_0^{\ell(x,\Omega)}\Big(e^{-\int_0^s\Sigma_t(x-s'\Omega)ds'}\Big)$$
$$\boldsymbol{\Omega} \cdot \Big[\boldsymbol{\nabla}\phi(\boldsymbol{x}) - 3\Sigma_{s1}(\boldsymbol{x} - s\boldsymbol{\Omega})\boldsymbol{J}(\boldsymbol{x})\Big]ds\,d\Omega$$
$$= -\frac{1}{4\pi}\int_{4\pi}\boldsymbol{\Omega}\Big(\int_0^{\ell(x,\Omega)}e^{-\int_0^s\Sigma_t(x-s'\Omega)ds'}ds\Big)\boldsymbol{\Omega}d\Omega \cdot \boldsymbol{\nabla}\phi(\boldsymbol{x})$$
$$+ \frac{3}{4\pi}\int_{4\pi}\boldsymbol{\Omega}\Big(\int_0^{\ell(x,\Omega)}e^{-\int_0^s\Sigma_t(x-s'\Omega)ds'}\Sigma_{s1}(\boldsymbol{x} - s\boldsymbol{\Omega})ds\Big)$$
$$\boldsymbol{\Omega}d\Omega \cdot \boldsymbol{J}(\boldsymbol{x})$$
$$= -\boldsymbol{M}_0(\boldsymbol{x}) \cdot \boldsymbol{\nabla}\phi(\boldsymbol{x}) + \boldsymbol{M}_1(\boldsymbol{x}) \cdot \boldsymbol{J}(\boldsymbol{x}) . \quad (16)$$

Here, the 3×3 tensor $\boldsymbol{M}_0(\boldsymbol{x})$ is defined by

$$\boldsymbol{M}_0(\boldsymbol{x}) = \frac{1}{4\pi}\int_{4\pi}\boldsymbol{\Omega}F_0(\boldsymbol{x}, \boldsymbol{\Omega})\boldsymbol{\Omega}\,d\Omega , \quad (17)$$

with $F_0(\boldsymbol{x}, \boldsymbol{\Omega})$ defined by

$$F_0(\boldsymbol{x}, \boldsymbol{\Omega}) = \int_0^{\ell(x,\Omega)}e^{-\int_0^s\Sigma_t(x-s'\Omega)ds'}ds . \quad (18a)$$

Equivalently [see Eqs. (8)], F_0 is defined by the simple transport problem:

$$\boldsymbol{\Omega} \cdot \boldsymbol{\nabla}F_0(\boldsymbol{x}, \boldsymbol{\Omega}) + \Sigma_t(\boldsymbol{x})F_0(\boldsymbol{x}, \boldsymbol{\Omega}) = 1 ,$$
$$\boldsymbol{x} \in V , \quad \boldsymbol{\Omega} \in 4\pi , \quad (18b)$$
$$F_0(\boldsymbol{x}, \boldsymbol{\Omega}) = 0 , \quad \boldsymbol{x} \in \partial V , \quad \boldsymbol{\Omega} \cdot \boldsymbol{n} < 0 . \quad (18c)$$

Also, the 3×3 tensor $\boldsymbol{M}_1(\boldsymbol{x})$ is defined by

$$\boldsymbol{M}_1(\boldsymbol{x}) = \frac{1}{4\pi}\int_{4\pi}\boldsymbol{\Omega}F_1(\boldsymbol{x}, \boldsymbol{\Omega})\boldsymbol{\Omega}\,d\Omega , \quad (19)$$

with $F_1(\boldsymbol{x}, \boldsymbol{\Omega})$ defined by

$$F_1(\boldsymbol{x}, \boldsymbol{\Omega}) = \int_0^{\ell(x,\Omega)}e^{-\int_0^s\Sigma_t(x-s'\Omega)ds'}\Sigma_{s1}(\boldsymbol{x} - s\boldsymbol{\Omega})ds . \quad (20a)$$

Equivalently [see Eqs. (8)], F_1 is defined by the simple transport problem:

$$\boldsymbol{\Omega} \cdot \boldsymbol{\nabla}F_1(\boldsymbol{x}, \boldsymbol{\Omega}) + \Sigma_t(\boldsymbol{x})F_1(\boldsymbol{x}, \boldsymbol{\Omega}) = 3\Sigma_{s1}(\boldsymbol{x}) ,$$
$$\boldsymbol{x} \in V , \quad \boldsymbol{\Omega} \in 4\pi , \quad (20b)$$
$$F_1(\boldsymbol{x}, \boldsymbol{\Omega}) = 0 , \quad \boldsymbol{x} \in \partial V , \quad \boldsymbol{\Omega} \cdot \boldsymbol{n} < 0 . \quad (20c)$$

Introducing the approximations (14b), (15b), and (16) into Eq. (13), we obtain

$$J(x) = -M_0(x) \cdot \nabla\phi(x) + M_1(x) \cdot J(x) .$$

This yields

$$J(x) = -D(x) \cdot \nabla\phi(x) , \qquad (21a)$$

where the diffusion tensor D is defined by

$$D(x) = (I - M_1(x))^{-1} \cdot M_0(x) . \qquad (21b)$$

Eqs. (17)-(21) are the principal results of this paper. Assuming that V is bounded, the functions $F_0(x, \Omega)$ and $F_1(x, \Omega)$ are bounded. Hence, the tensors $M_0(x)$ and $M_1(x)$ are bounded for all points $x \in V$, even for points within a void region. Eqs. (3) and (21a) describe the new diffusion approximation, with the non-local diffusion tensor D. The vacuum boundary conditions (18c) and (20c) for F_0 and F_1 are important new features of our analysis that were not derived previously.

As a simple check, if V is infinite and homogeneous, then Eq. (18b) gives:

$$F_0(x, \Omega) = \frac{1}{\Sigma_t} \quad , \quad M_0 = \frac{1}{3\Sigma_t}I , \qquad (22a)$$

Eq. (20b) gives:

$$F_1(x, \Omega) = \frac{3\Sigma_{s1}}{\Sigma_t} \quad , \quad M_1 = \frac{\Sigma_{s1}}{\Sigma_t}I , \qquad (22b)$$

and Eq. (21b) yields:

$$D = \left(I - \frac{\Sigma_{s1}}{\Sigma_t}I\right)^{-1} \cdot \frac{1}{3\Sigma_t}I = \frac{1}{3(\Sigma_t - \Sigma_{s1})}I . \qquad (22c)$$

This is the standard (scalar) diffusion coefficient.

IV. COMPUTATIONAL RESULTS

A study of the accuracy of our theory for 3D anisotropic scattering problems is not possible at the present time. However, it is possible for us to compare diffusion tensors generated assuming anisotropic scattering, with those generated by assuming isotropic scattering with a transport-corrected total cross section. The former corresponds to using Eq. (21b) for the diffusion tensor, while the latter corresponds to using Eq. (17) for the diffusion tensor, with the total cross section replaced in that equation by the transport-corrected total cross section.

We have performed calculations for three problems to demonstrate the differences between these two tensors. The first problem corresponds to a homogeneous non-absorbing 2-D domain 10 *cm* in length on a side. The scattering section is 1 cm^{-1}, and the transport-corrected scattering cross section is 0.5 cm^{-1}. This corresponds to P_1 anisotropic scattering with $\sigma_0 = 1$ cm^{-1} and $\sigma_1 = 0.5$ cm^{-1}, or isotropic scattering with $\sigma_0 = 0.5$ cm^{-1}. The second problem differs from the first only in that there is a square void 1 *cm* in length on a side embedded at the center of the domain, as shown in Fig. 2. The third problem differs from the second only in that the void is

located adjacent to the center of a boundary face as shown in Fig. 3. A weighted-diamond difference scheme is used to spatially discretize Eqs.(18b) and (20b). Vacuum boundary conditions are used in the calculations as indicated by Eqs.(18c) and (20c). For all calculations, a Gauss-Chebyshev S_8 quadrature set is used and each cell has a thickness of 0.01 *cm*.
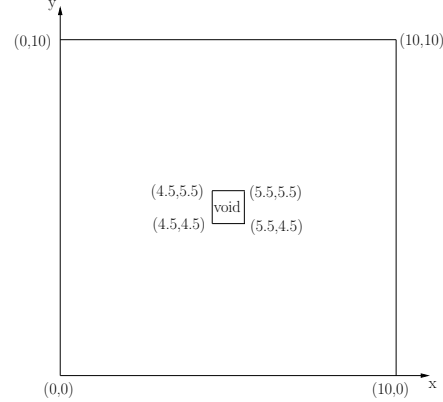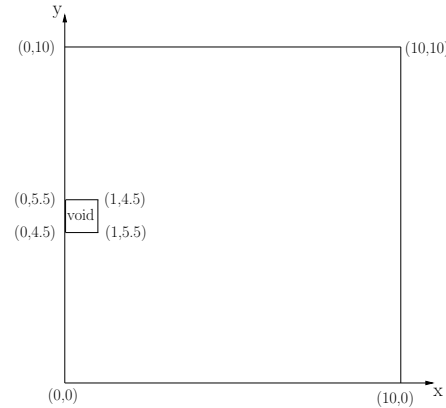

Fig. 2: Problem 2 Geometry.

Fig. 3: Problem 3 Geometry.

The calculated diffusion tensor elements D_{xx}, D_{yy} and D_{xy}, for Problem 1 using Eq. (21b), are plotted in Fig. 4. The same scale is used in Figs. 4a and 4b, and a scale of -0.08 to 0.08 is used in Fig. 4c. The values of D_{xx} and D_{yy} in the center of the geometry are close to 0.66, as expected. From Fig. 4c, it can be found that the values of D_{xy} are close to zero except on the boundary corners. The diffusion tensor elements D_{xx}, D_{yy} and D_{xy}, at the cut plane $y = 5$ *cm* generated by using Eq. (21b) or using Eq. (17) with a transport-corrected total cross section, are plotted in Fig. 5. The values of D_{xx} generated using Eq. (21b) are slightly larger than the ones generated using Eq. (17) except the latter become slightly larger than the former near the boundaries. Similar results are observed in Fig. 5b. In Fig. 5c, there is negligible difference between the values of D_{xy} generated using Eq. (21b) or Eq. (17), but the values are essentially zero.

The calculated diffusion tensor elements D_{xx}, D_{yy} and D_{xy}, for Problem 2 using Eq. (21b), are plotted in Fig. 6. The
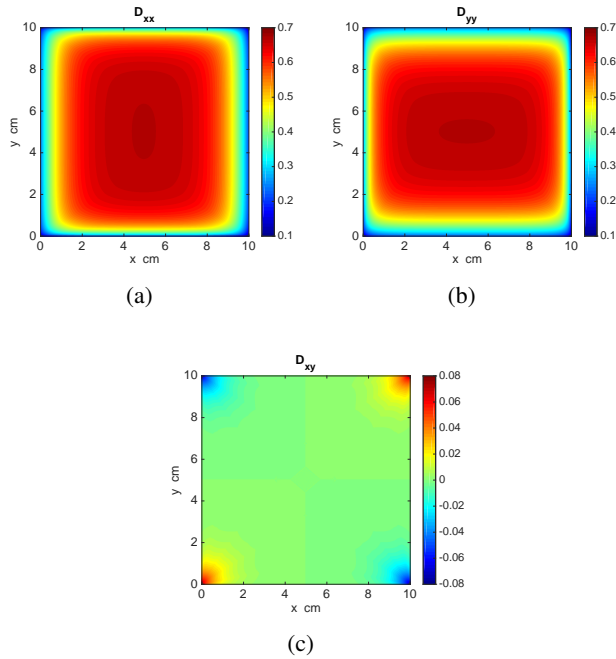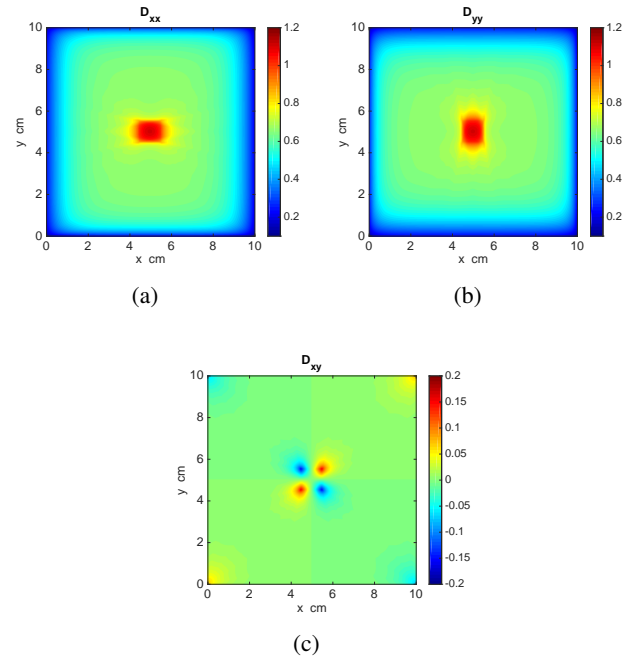
Fig. 4: The diffusion tensor calculated for Problem 1.

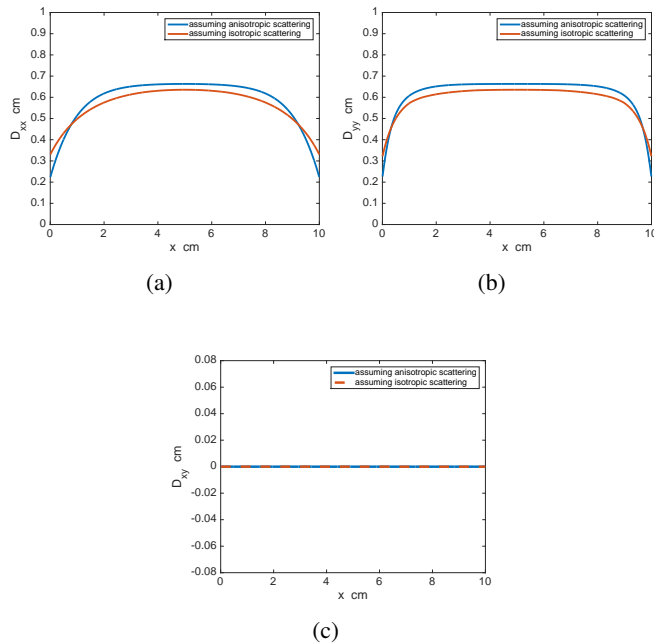Fig. 6: The diffusion tensor calculated for Problem 2.

Fig. 5: The diffusion tensor for Problem 1 at the cut plane $y = 5$ *cm* generated by assuming anisotropic scattering or isotropic scattering with a transport-corrected total cross section. The former is colored in blue, and the latter is colored in orange.

Fig. 7: The diffusion tensor for Problem 2 at the cut plane $y = 5$ *cm* generated by assuming anisotropic scattering or isotropic scattering with a transport-corrected total cross section. The former is colored in blue, and the latter is colored in orange.

maximum and minimum values of D_{xx} and D_{yy} in the void are about 1.11 and 0.88, respectively. In Fig. 6c, it is observed
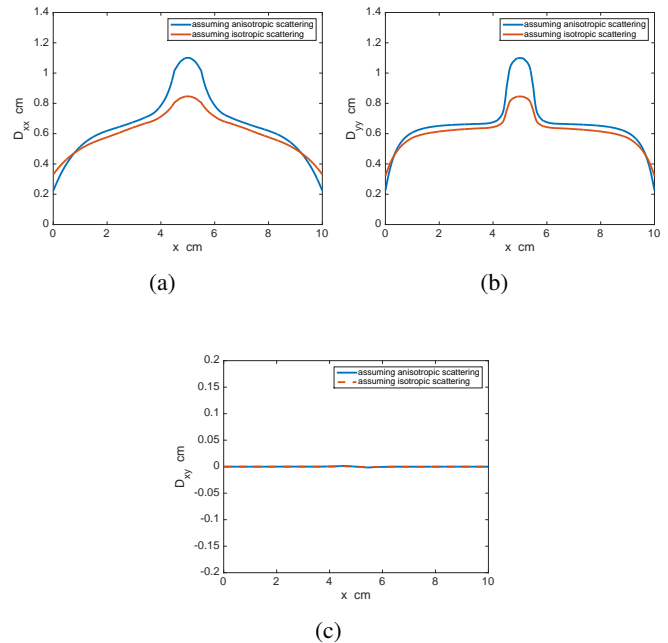
that the values of D_{xy} are close to zero except at the void corners and material corners. The diffusion tensor elements

D_{xx}, D_{yy} and D_{xy}, at the cut plane $y = 5\ cm$ generated by using Eq. (21b) or using Eq. (17) with a transport-corrected total cross section, are plotted in Fig. 7. In Fig. 7a the values of D_{xx} generated using Eq. (21b) are much larger than the ones generated using Eq. (17) in the void while the latter become slightly larger than the former near the material boundary. Similar results are observed in Fig. 7b. In Fig. 7c, there is negligible difference between the values of D_{xy} generated using Eq. (21b) or Eq. (17), but the values are nearly zero.

The calculated diffusion tensor elements D_{xx}, D_{yy} and D_{xy}, for Problem 3 using Eq. (21b), are plotted in Fig. 8. The values of D_{yy} in the void are larger than D_{xx}, as expected. The maximum values of D_{xx} and D_{yy} in the void are about 0.56 and 0.85, respectively, while the minimum values of D_{xx} and D_{yy} in the void are almost the same, about 0.37. From Fig. 8c, it can be found that the values of D_{xy} are close to zero except near the boundaries of the void and material corners. The diffusion tensor elements D_{xx}, D_{yy} and D_{xy}, at the cut plane $y = 5\ cm$ generated by using Eq. (21b) or using Eq. (17) with a transport-corrected total cross section, are plotted in Fig. 9. In Fig. 9a, the values of D_{xx} generated using Eq. (21b) are slightly larger than the ones generated using Eq. (17) except the latter become slightly larger in the void and near the material boundaries. However, in Fig. 9b, the values of D_{yy} generated using Eq. (21b) are much larger than the ones generated using Eq. (17) in the void. In Fig. 9c, there is negligible difference between the values of D_{xy} generated using Eq. (21b) or Eq. (17), but the values are essentially zero.

These results show that for neutron transport problems with anisotropic scattering, there can be a significant difference between the nonlocal diffusion tensors calculated using (i) the systematic nonlocal anisotropic-scattering theory presented here, or (ii) using the familiar transport-corrected isotropically-scattering cross sections with the nonlocal isotropically-scattering theory. The differences are due to the fact that the standard transport-corrected cross sections arise using the conventional P_1 or diffusion approximation, which is not valid in regions with voids.

Unfortunately, it is not at the present time possible for us to assess the accuracy of solutions of 3D anisotropically-scattering problems with voids using the new theory. This assessment will be done in future work.

V. DISCUSSION

The analysis in this paper shows that if the proper conditions are met, and proper care is taken, it is theoretically possible to accurately model – using diffusion theory – a neutronic system containing voids. The price to be paid is that the normally "scalar" diffusion tensor

$$D = \frac{1}{3\Sigma_{tr}}I \qquad (23)$$

becomes a 3×3 tensor, and the coefficients of this tensor must be calculated by solving two transport problems. Fortunately, these problems are considerably simpler and less expensive to solve than the original transport problem for ψ.

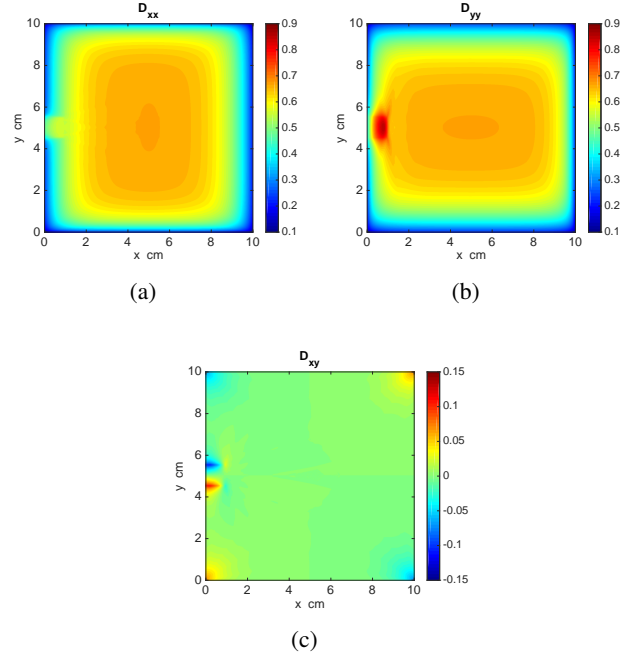It is physically correct that D should become nonscalar

(a)

(b)

(c)

Fig. 8: The diffusion tensor calculated for Problem 3.

(a)

(b)

(c)

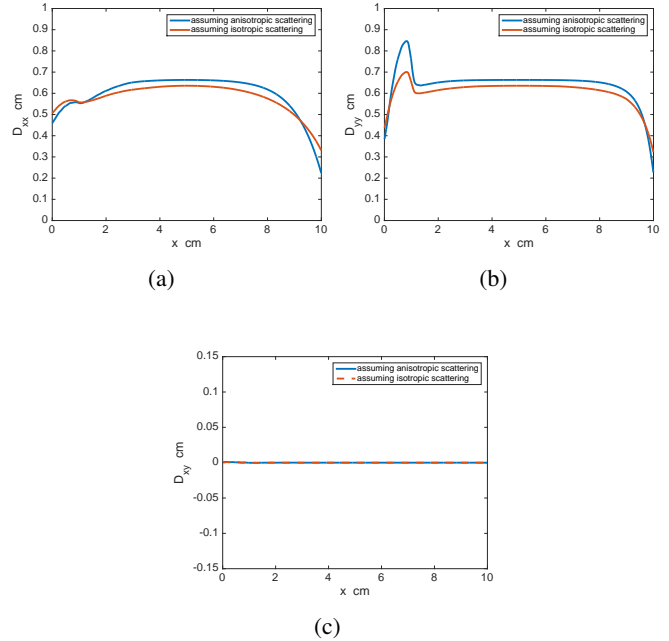Fig. 9: The diffusion tensor for Problem 3 at the cut plane $y = 5\ cm$ generated by assuming anisotropic scattering or isotropic scattering with a transport-corrected total cross section. The former is colored in blue, and the latter is colored in orange.

in a void region. If the void is a narrow channel, then neutrons in the channel, streaming in directions parallel to the

channel, will travel long distances between collisions, while neutrons streaming in directions perpendicular to the channel will travel short distances between collisions. The rates at which neutrons propagate in the two directions are different, and the nonlocal diffusion tensor should reflect this fact.

A specific numerical issue must be considered before applying the theory outlined in this paper. For problems with systems having narrow voided channels, $\psi(x, \Omega)$ [the solution of Eqs. (1)] does not have a simple dependence on x and Ω for points x near a channel. The same is true for the functions $F_0(x, \Omega)$ [the solution of Eqs. (18)] and $F_1(x, \Omega)$ [the solution of Eqs. (20)]. If an accurate deterministic numerical solution of Eqs. (1) for ψ is desired, then it will be necessary to use a suitably fine spatial grid near the channels and a fine angular grid (at least, in the necessary directions of flight in the channel directions). The same is also true for deterministic calculations of F_0 and F_1.

Therefore, there is no simple escape from all the difficulties introduced by voided channels; the only "partial" escape is that single transport sweeps are required to determine F_0 and F_1, whereas many sweeps are generally required to calculate ψ. Also, after F_0, F_1, and D have been calculated, D will have a rapid spatial (i.e. "boundary layer") behavior near void regions. Thus, in the diffusion calculation, there is no escape from the necessity of using a fine spatial grid near the voided channels.

The basic message is that certain diffusive problems containing voids can be treated using diffusion theory – but not surprisingly – the attainment of accurate results requires more computational effort than is required for problems without voids. Also, due to the current lack of 3D computational results, it is not yet clear how accurate the new theory will be for problems of practical interest (e.g. fast reactors, which have "1D" voids; and TREAT, which has a major "2D" void in the hodoscope region).

While it is possible to approximately account for anisotropic scattering with the transport-corrected isotropic scattering, our simple calculations indicate that the difference between the resulting diffusion tensors in void can be significant and may not be neglected. In future work, we will quantify the differences in solutions for practical 3D problems between the anisotropic and transport-corrected isotropic approaches.

Finally, this paper establishes a more complete theoretical basis for the method now being considered to simulate TREAT. During the implementation of the method in INL codes, the question of boundary conditions on ∂V for F_0 and F_1 arose. In the previous publications [4, 5, 6], V was assumed to be infinite, and no finite boundary conditions for F_0 and F_1 were derived. In [6], it was speculated that reflecting boundary conditions should be used, and these were tried at INL. However, vacuum boundary conditions were also tried, and were found to yield improved results [7]. The vacuum boundary conditions for F_0 and F_1 derived in this paper [Eqs. (18c) and (20c)] provide a theoretical explanation for this experimentally-observed result.

The extension of the theory in this paper to time-dependent, multigroup problems is straightforward if scattering is isotropic. However, multigroup problems with anisotropic scattering pose certain difficulties that have not been fully resolved. These will be addressed in future work.

VI. ACKNOWLEDGMENTS

REFERENCES

1. N.L. Laletin, "The Effect of a Cylindrical Channel on Neutron Diffusion," *J. Nucl. Energy. Part A: Reactor Science*, **13**, 57 (1960).
2. R.N. Hwang, "Effect of Cavities on Neutron Diffusion," Ph.D. Thesis, Iowa State University of Science and Technology, Ames, Iowa (1962).
3. H. Gerwin and W. Scherer, "Treatment of the Upper Cavity in a Pebble-Bed High-Temperature Gas-Cooled Reactor by Diffusion Theory," *Nucl. Sci. Eng.* **97**, 9 (1987).
4. J.E. Morel, "A Non-Local Tensor Diffusion Theory," Los Alamos National Laboratory Report LA-UR-07-5257 (2007).
5. J.E. Morel, J.S. Warsa, and K.G. Budge, "Alternative Generation of Non-Local Diffusion Tensors," Los Alamos National Laboratory Report LA-UR-10-08285 (2010).
6. T.J. Trahan and E.W. Larsen, "3-D Anisotropic Neutron Diffusion in Optically Thick Media with Optically Thin Channels," *Proc. Int. Conf. on Math. and Comp. Methods Applied to Nuclear Science and Eng. (M&C 2011)*, Rio de Janeiro, RJ, Brazil, May 8-12, 2011, American Nuclear Society (2011).
7. S. Schunert, H. Hammer, J. Lou, Y. Wang, J. Ortensi, F. Gleicher, B. Baker, M. DeHart, and R. Martineau, "Using Directional Diffusion Coefficients for Nonlinear Diffusion Acceleration of the First Order S_N Equations in Near-Void Regions," *Trans. Am. Nucl. Society,* to appear (Winter, 2016).